Charm quark energy loss in infinite QCD matter using a parton cascade model

Mohammed Younus, Christopher E. Coleman-Smith, Steffen A. Bass, and Dinesh K. Srivastava

Charm Quark Energy Loss In Infinite QCD Matter Using a Parton Cascade Model

Mohammed Younus,[1, *] Christopher E. Coleman-Smith,[2] Steffen A. Bass,[2, †] and Dinesh K. Srivastava[1, ‡]

[1]*Variable Energy Cyclotron Centre, 1/AF Bidhan Nagar Road, Kolkata 700064, INDIA*
[2]*Duke University, Dept. of Physics, 139 Science Drive, Box 90305, Durham NC 27708, U. S. A.*

We utilize the Parton Cascade Model to study the evolution of charm quarks propagating through a thermal brick of QCD matter. We determine the energy loss and the transport coefficient '$\hat{q}$' for charm quarks. The calculations are done at a constant temperature of 350 MeV and the results are compared to analytical calculations of heavy quark energy loss in order to validate the applicability of using a Parton Cascade Model for the study of heavy quarks dynamics in hot and dense QCD matter.

I. INTRODUCTION

Relativistic heavy ion collision at RHIC and the LHC have given rise to a new phase of matter. When two heavy ions collide, a system of deconfined gluons and quarks within a very small volume is created. The initial energy density within this volume is found to be on the order of 30 GeV/fm^3. This state of matter as we know today is called quark gluon plasma [1, 2]. The study of QGP is particularly important as it aims to produce a condition which resembles the period when universe was only a few microseconds old. However, since this exotic system created in the experiments exists only for a very short period of time and is not directly observable, only signals originating from the matter itself that survive and are measured after the collisions can provide a window into the nature of the QGP [3, 4].

One of the prominent signatures coming out of the QGP phase is jet quenching: High momentum hadron spectra are observed to be highly suppressed relative to those in proton on proton collisions [5, 6], suggesting a quenching effect due to deconfined matter. A similar effect is observed for high p_T charm or beauty quarks with most recent results showing suppression of D or B mesons to same order as that of light partons [7]. Calculations from hydrodynamics also give a rough estimate of the ratio of thermalization time for heavy quarks and light partons [8], $\frac{\tau_Q}{\tau_{q/g}} \sim \frac{M_Q}{T}$. For $M_Q = 1.35$–4.5 GeV and T = 300 MeV, this ratio is found to be$\sim$ 5 and suggests that relaxation time for heavy quarks is larger than that of light quarks and gluons. If thermalization time, $\tau_{q/g}$, is taken to be $\mathcal{O}(1\text{fm/c})$, and if equilibrium temperature, T_i and freeze-out temperature, T_f are taken as 300 MeV and 170 MeV [9] respectively, then the lifetime of the QGP can be approximately shown to be 5 fm/c. This might imply that the heavy quark relaxation time for T= 300 MeV is comparable to the QGP lifetime at this condition. Even if the heavy quark is subjected to large suppression [7], it may not fully thermalize in the QGP. Overall,

*Electronic address: younus.presi@gmail.com
†Electronic address: bass@phy.duke.edu
‡Electronic address: dinesh@vecc.gov.in

the study of heavy quark dynamics is slowly emerging as one of the most active fields of research in heavy ion collision physics.

Various theoretical calculations and phenomenological models of heavy quarks energy loss have appeared in recent years [10]–[15]. Elastic scattering and inelastic gluon emission are the major mechanisms by which a heavy quark may lose energy in the presence of a thermal medium. In most of these earlier works, collisional energy loss seems to dominate in the lower momentum region while radiative energy loss emerges as the chief mechanism for higher momenta charms.

Transport models attempt to fully describe the dynamics of the time-evolution of a heavy ion collision. The Parton Cascade Model is one such model [16–18]. It is based on the Boltzmann Equation and does not include any equilibration assumptions. However the calculations must be well calibrated and validated under controlled conditions before utilizing them for meaningful predictions. Performing this validation for the medium evolution of heavy quarks is the purpose of this work.

II. PARTON CASCADE MODEL

The Parton Cascade Model VNI/BMS [19–21] forms the basis for our present study. This model can be used to study the full time evolution of hard probes in a thermal QCD medium. The PCM has been used to study gluons and lighter quarks as hard probes of the QGP. In the current work we use VNI/BMS to study the evolution of charm quarks in an infinite QGP medium for the first time. The purpose of this study is to provide a verifiable benchmark calculation to validate the model and subsequently apply it to the more complex and dynamic regime of a heavy-ion collision.

The infinite QGP medium is modeled by taking a box of finite volume with periodic boundary conditions. This provides a system of infinite matter at fixed temperature. The matter inside the box consists of thermalized quarks and gluons (QGP) which are being generated using thermal distributions at a given temperature and zero chemical potential. We insert a charm quark with the four momentum $p^\mu = \{0, 0, p_z, E = \sqrt{p_z^2 + M_c^2}\}$, into the box and let it evolve according to the Relativistic Boltzmann

Equation given by,

$$p^\mu \frac{\partial F_k(x, \vec{p})}{\partial x^\mu} = \sum_{processes:i} C_i[F],\qquad(1)$$

where $F_k(x, \vec{p})$ is the single particle phase space distribution and the collision term on r.h.s. is a non-linear functional of phase space distribution terms inside an integral.

We have included the matrix elements for all $2 \to 2$ binary elastic scattering processes for charm interaction with gluons or light quarks(u, d, s) and $2 \to n$ process for radiative (brehmsstrahlung) corrections after each scattering.

A. Elastic scattering of charm quark

The elastic processes included are

$$cg \to cg,\qquad(2)$$
$$cq(\bar{q}) \to cq(\bar{q}).$$

The corresponding differential scattering cross section is defined to be,

$$\frac{d\hat{\sigma}}{dQ^2} = \frac{1}{16\pi(\hat{s} - M_c^2)^2} \sum |\mathcal{M}|^2.\qquad(3)$$

The total cross section is also calculated and used in the calculations to select interacting pairs. The total cross section can be shown to be,

$$\hat{\sigma}_{tot} = \sum_{c,d} \int_{p_{Tmin}^2}^{\hat{s}} \left(\frac{d\hat{\sigma}}{dQ^2}\right)_{ab \to cd} dQ^2.\qquad(4)$$

The invariant transition amplitudes, $|\mathcal{M}|^2$ for elastic scattering which can be calculated or obtained from [22], are shown below for $q(\bar{q})c \to q(\bar{q})c$,

$$\sum |\mathcal{M}|^2 = \frac{64\pi^2\alpha_s^2}{9} \frac{(M_c^2 - \hat{u})^2 + (\hat{s} - M_c^2)^2 + 2M_c^2\hat{t}}{(\hat{t} - \mu_D^2)^2}.$$
$$(5)$$

While, for $gc \to gc$,

$$\sum |\mathcal{M}|^2 = \pi^2\alpha_s^2[g1 + g2 + g3 + g4 + g5 + g6],$$

$$g1 = 32\frac{(\hat{s} - M_c^2)(M_c^2 - \hat{u})}{(\hat{t} - \mu_D^2)^2},$$

$$g2 = \frac{64}{9}\frac{(\hat{s} - M_c^2)(M_c^2 - \hat{u}) + 2M_c^2(\hat{s} + M_c^2)}{(\hat{s} - M_c^2)^2},$$

$$g3 = \frac{64}{9}\frac{(\hat{s} - M_c^2)(M_c^2 - \hat{u}) + 2M_c^2(M_c^2 + \hat{u})}{(M_c^2 - \hat{u})^2},$$

$$g4 = \frac{16}{9}\frac{M_c^2(4M_c^2 - \hat{t})}{(\hat{s} - M_c^2)(M_c^2 - \hat{u})},$$

$$g5 = 16\frac{(\hat{s} - M_c^2)(M_c^2 - \hat{u}) + M_c^2(\hat{s} - \hat{u})}{(\hat{t} - \mu_D^2)(\hat{s} - M_c^2)},$$

$$g6 = -16\frac{(\hat{s} - M_c^2)(M_c^2 - \hat{u}) - M_c^2(\hat{s} - \hat{u})}{(\hat{t} - \mu_D^2)(M_c^2 - \hat{u})}.\qquad(6)$$

In order to regularize the cross sections we have used the thermal mass of QGP medium which is defined as $\mu_D = \sqrt{(2N_c + N_f)/6}gT$, where $g = \sqrt{4\pi\alpha_s}$ and α_s is the strong coupling constant. N_f, no. of flavours and N_c, no. of colours are taken 4 and 3 respectively. We have kept α_s=0.3 fixed for the entire calculation. While the PCM has the capability of using a running or temperature-dependent coupling constant, keeping it a fixed value allows us to easily compare our calculations to analytic expressions for the same quantities, which is the main purpose of the present work.

The Boltzmann transport equation is then solved numerically via Monte Carlo algorithms, a geometric interpretation of the cross section is used to select which collisions will occur.

B. Charm Quark Radiation

It is known that collisional loss alone is unable to explain the data showing suppression of D mesons at LHC [23]. On the one hand, the hard thermal loop(HTL) approximation [24, 25] predicts a large drag on heavy quarks which is much bigger than what experimental data has suggested, while the radiative corrections to heavy quark energy loss when combined with elastic scattering are able to explain the results agreeably [23].

In our calculations, radiative corrections are included in form of time-like branching of the probe charm into a final charm and a shower of radiated partons using Altarelli-Parisi(AP) splitting function [26]. The basic idea is that during a binary scattering the outgoing partons may acquire some virtuality. These partons are allowed to radiate a shower of partons until their virtuality decreases to some preassigned cutoff value, μ_0^2 ($\approx M_c^2$ for charm quarks).

Any quark subjected to multiple collision may radiate a shower of partons as has been discussed earlier [27–29]. However emission of multiple partons within a certain length scale may lead to a reduction of the

bremsstrahlung cross-sections which we can briefly discuss here. This reduction in emitted gluon spectrum is known as Landau Pomeranchuk Migdal (LPM) effect [30]. This arises from the fact that if the formation time of an emitted gluon after a $Qq(Qg)$ scattering is larger than the typical mean free path of the heavy quark itself, then a gluon emitted from the next scattering centre may interact coherently with the initial gluon. This interference of emitted gluons may continue if there are a number of scattering centres before the shower of gluons dissociates itself completely from the emitting parton. Radiative energy loss via the LPM effect has previously been calculated for heavy quarks by [31, 32]. The LPM effect in radiative corrections to charm quark energy loss has been utilized to describe the observed suppression of single non-photonic electrons [13].

In the PCM, the LPM effect has been implemented using a MC algorithm [33] first proposed by Zapp and Wiedemann [34]: This method is particularly appealing since it requires no artificial parametrization of the radiative process, it is a purely probabilistic medium induced modification.

After the production of a parton shower via an inelastic collision, the hardest radiated gluon is selected to represent the shower as the probe and re-interact with the medium. This reflects the dominance of the gluon rescattering in the interference process. The formation times

$$\tau_f^0 = \sum_{branchings} \frac{\omega}{\mathbf{k}_\perp^2}, \tag{7}$$

for each branching during the parton shower leading up to the production of the probe gluon are summed. The heavy quark is allowed to propagate through the medium and rescatter elastically during this time, the remainder of the partons from the radiation event propagate spatially but may not interact. Each time the probe gluon rescatters its formation time is recalculated as

$$\tau_f^n = \frac{\omega}{\left(\mathbf{k}_\perp + \sum_{i=1}^n \mathbf{q}_{\perp,i}\right)^2}. \tag{8}$$

this simulates the emission of the shower from n centers which transfer their momentum coherently. After this formation time expires the radiation is considered to have separated from the initiating heavy quark and all partons may once again interact and radiate.

III. RESULTS AND DISCUSSION

In our calculations we have set the strong coupling constant to a fixed value of $\alpha_s = 0.3$ to allow comparison with analytical calculations and other transport models. The temperature is set to T=350 MeV, which is roughly the average temperature of the QGP phase attained at RHIC energies. The mass of charm is taken as $M_c = 1.35$ GeV. For future applications of our model to
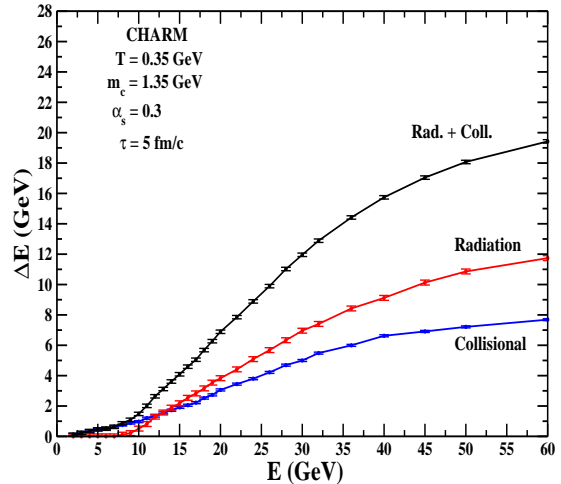

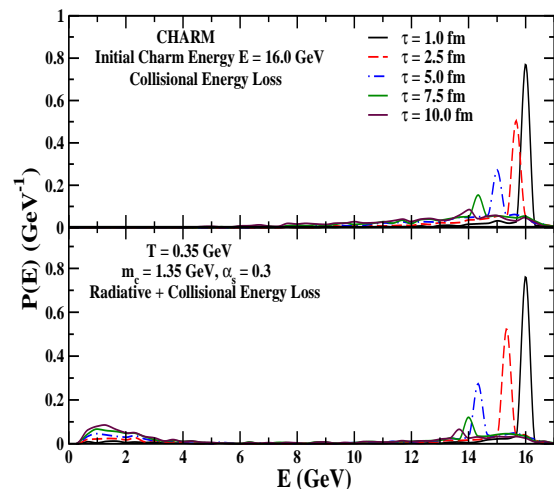FIG. 1: (Color online)Energy loss for different initial charm energies after 5 fm/c of propagation.

FIG. 2: (Color online)Energy profile for 16 GeV charm for different time

nucleus-nucleus collisions we shall use a running coupling constant instead.

In Fig: 1, we show energy loss,'ΔE', of charm quark over a given path length($L \sim 5 fm$) as a function of its initial energy. For discussions on path length dependence of energy loss evolution, other figures in this paper will be referred next.

We may now return to Fig: 1 for detailed discussions. The loss due to elastic scattering, radiation and total loss are shown separately in the same figure. We may observe that collisional loss dominates over radiation up to $7-12$ GeV of initial charm energy, and beyond this energy regime, charm quark radiation dominates and con-
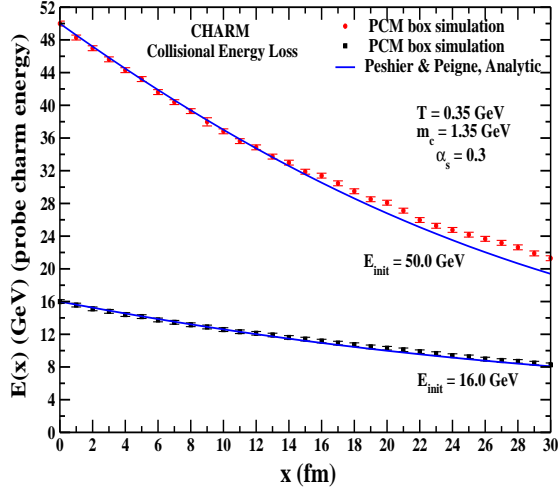
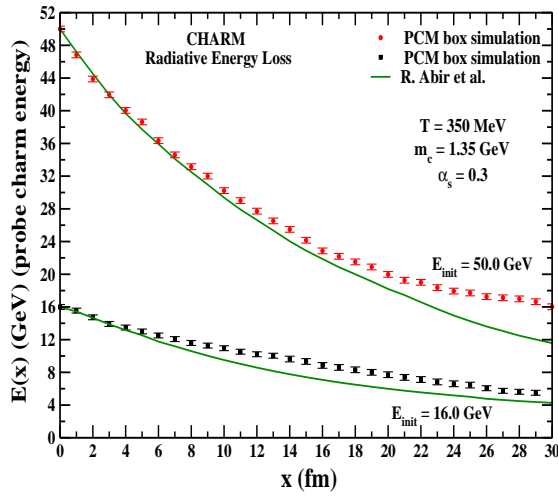FIG. 3: (Color online)Energy of probe charm with distance traveled for elastic scattering only

FIG. 4: (Color online)Energy of probe charm with distance traveled for radiative energy loss only

tributes more towards the energy loss. However the radiation too appears to decrease for very high energy charms which may be the factor behind the decrease in charm quark suppression in high momentum regions. With increasing initial energy of the charm quark, the rise in energy loss(both collisional and radiative) over the 5 fm length appears to level off – we can see this in particular prominent for elastic energy loss. We feel that as momentum of charm increases, the average no. of elastic scattering tends to saturate so that the collisional energy loss tends to saturate. But let us recall that in our case, radiation takes place only after elastic scattering, and as the no. of scattering saturates ultimately,

so does the radiative loss for very high energy charm quarks. This particular trend may be reflected in the decrease of nuclear suppression factor, R_{AA}, of heavy quark in the final heavy meson spectra at high momentum region [7]. Our findings are consistent with e.g. [8], where it was discussed that for small coupling, α_s, collisional loss tends to dominate for low and intermediate energy charm(for $\gamma v_Q \sim 1$, $\gamma = (1 - \beta^2)^{-1/2}$) while for higher energetic heavy quarks we have bremsstrahlung (for $\gamma v_Q \sim 1/g$, $g = \sqrt{4\pi\alpha_s}$) dominating over collisional energy-loss. Other discussions on the topic are given in [35].

In Fig: 2 we show the energy profile of a 16 GeV charm after several time intervals of propagation through the thermal medium. Here $P(E)$ can be defined as $= \frac{1}{N}\frac{dN}{dE}$. The energy loss due to collisional and collisional+radiative processes is shown separately in the same figure. The collisional loss (upper panel) shows a shift in the position of the peak with long tail like structure extending towards the low energy regions. A recent study of charm quark energy profile using a Langevin equation along with a hydrodynamical background has instead shown a more Gaussian like distribution [36]. Some other discussions on the differences between Boltzmann and Langevin equations for heavy quark dynamics are also given in [36]. Additionally we find that inclusion of radiative corrections brings about a significant change in the profile and indicates that for high energy charm quarks the effect of radiative loss is much greater than collisional loss, with the bulk of of 16.0 GeV charm quarks ultimately shifting to very low energy(< 2.0 GeV) regions after 10 fm.

Next we study the evolution of charm quark energy as a function of distance traveled through the medium in Fig: 3 and Fig: 4. The calculation uses two different initial energies (16 GeV and 50 GeV respectively) for charm. Collisional loss and radiative loss are shown in these two figures separately – the radiative energy-loss figure was obtained by subtracting the elastic energy-loss calculation from the full calculation that included collisional+radiative energy-loss. We would like to elucidate the fact that these two diagrams show energy of charm quark after each 'fm' of path length traversed and shows the path length behaviour of charm quark. These plots may be used to give the total energy loss of charm for comparison to Fig: 1.

Now let us discuss Figs. Fig: 3 and Fig: 2 in detail. The curves for the 50 GeV charm quarks show a clear distinction between the radiative and collisional energy-loss mechanisms: whereas the collisional energy-loss shows initially a linear behavior, the radiative energy-loss leads to a much stronger, near quadratic, fall-off in the energy for the first 20 fm/c. For the charm quarks with an initial energy of 16 GeV the differences are far less pronounced, but even here a ratio between the two curves would yield interesting differences. For both cases, we compare our results to analytical calculations of dE/dx. For collisional loss we have used an analytical form by

Peshier and Peigne [37] which can be written as:

$$\frac{dE}{dx} = \frac{4\pi\alpha_s^2 T^2}{3}\left[\left(1 + \frac{N_f}{6}\right) \cdot \right.$$
$$\left. \ln\frac{E_p(x)T}{\mu_D^2} + \frac{2}{9}\ln\frac{E_p(x)T}{M_c^2} + c(N_f)\right]$$

$$(9)$$

Both for our PCM calculation as well as for the analytical expression we have used the following values for the parameters in order to compare the two. They are: a medium temperature of T= 350 MeV (applicable for RHIC-QGP system), a charm mass of M_c=1.35 GeV, no. of flavours and colours, N_f=4, N_c=3, a fixed coupling strength of $\alpha_s = 0.3$, and a screening mass $\mu_D = \sqrt{(2N_c + N_f)/6}gT$. We find that for the above set of parameters, the PCM results show good agreement to the predictions from the analytical expression, validating our computational setup and approach.

Next we move over to results on charm quark radiative energy loss Fig: 4. The radiative energy loss is compared to an analytical calculation by R. Abir et al [38] shown below:

$$\frac{dE}{dx} = 24\alpha_s^3\left(\rho_q + \frac{9}{4}\rho_g\right)\frac{1}{\mu_g}(1 - \beta_1)$$
$$\times \left(\frac{1}{\sqrt{(1 - \beta_1)}}[\log(\beta_1)^{-1}]^{1/2} - 1\right)\mathcal{F}(\delta)$$

where

$$\mathcal{F}(\delta) = 2\delta - \frac{1}{2}\log\left(\frac{1 + M_c^2 e^{2\delta}/s}{1 + M_c^2 e^{-2\delta}/s}\right)$$
$$- \frac{M_c^2 \cosh\delta/s}{1 + 2M_c^2\cosh\delta/s + M_c^4/s^2},$$
$$\delta = \frac{1}{2}\log\left[\frac{\log\beta_1^{-1}}{(1 - \beta_1)}\left(1 + \sqrt{1 - \frac{(1 - \beta_1)^{1/2}}{[\log\beta_1^{-1}]^{1/2}}}\right)^2\right],$$
$$s = E^2(1 + \beta_0)^2, \; \beta_1 = \frac{g^2}{C}\frac{T}{E}, \; \beta_0 = (1 - M_c^2/E^2)^{1/2},$$
$$C = \frac{3}{2} - \frac{M_c^2}{4ET} + \frac{M_c^4}{48E^2T^2\beta_0}\log\left[\frac{M_c^2 + 6ET(1 + \beta_0)}{M_c^2 + 6ET(1 - \beta_0)}\right]$$

$$(10)$$

As in the elastic energy-loss case, we have used identical values for parameters in the PCM calculation and in the analytic case, such as T =350 MeV, M_c= 1.35 GeV, α_s= 0.3, N_f=4, N_c= 3 and $\mu_D = \sqrt{(2N_c + N_f)/6}gT$.

Note, however, that the calculations of [38] is carried out in the Bethe-Heitler limit of radiative energy loss with the effects of the dead-cone formalism being explicitly included in the calculation. The authors of [38] state that the LPM effect if added would only affect a marginal change in the final gluon emission spectrum which is clearly not what our results suggest. The PCM simulation explicitly takes the LPM effect into account as discussed in the previous sections. We do find that our simulation results for coherent gluon emission of charm quarks agrees reasonably well to that of the analytical calculation upto $x = 5$–6 fm, supporting the claim that modifications to the heavy-quark emission spectrum due to the LPM effect for this particular medium length, are modest. For $x > 6$ fm, however, the simulation result involving LPM effect and analytical curve in the BH limit move apart from each other. When we change the energy of charm probe, E_c, from 16 GeV to 50 GeV, the differences between BH and LPM radiative mechanisms increase and become more profound and visible. This may be indicative of the rising importance of the coherent gluon emission effects at higher charm quark energies. We would also like to highlight our choice of parameter, N_f= 4, which introduces an 10% uncertainty in the total interaction cross-section assuming that the medium partons in our calculations are massless.

Overall we are confident that the comparison and agreement between PCM and the analytical calculations validates the PCM approach to heavy-quark energy loss and allows us to utilize the PCM for observables and calculations that are beyond the scope of analytical approaches, e.g. in the rapidly evolving non-equilibrium domain of ultra-relativistic heavy-ion collisions.

Next let us move over to our calculation of transverse momentum broadening per unit length of charm quarks also known as the transport coefficient $\hat{q}$ [39, 40]. In other words $\langle\hat{q}\rangle$ is a jet-quenching parameter calculated as a measure of momentum broadening within various energy loss models. Also the term 'transverse' refers to the direction perpendicular to the original direction of propagation and consequently for a jet of partons in the medium, the average or mean momentum of the jet remains unchanged while the momenta of each parton show broadening resulting in the redistribution of the transverse momentum spectrum of the jet partons. Some recent calculations have suggested values of this coefficient ranging from 0.5–20 GeV^2/fm [41] for light quarks. For heavy quarks, it was calculated in [42] which showed the value of $\hat{q} \sim 0.3$–0.7 GeV^2/fm. More detailed discussions and recent results on $\hat{q}$ of partons and heavy quarks can be found in [43, 44].

Generally, the transport coefficient $\hat{q}$ can be defined as:

$$\frac{d(\Delta p_T^2)}{dx} = \hat{q} = \rho\int d^2 q_\perp q_\perp^2 \frac{d\sigma}{d^2 q_\perp} \qquad (11)$$

where $\frac{d\sigma}{d^2 q_\perp}$ is the differential scattering cross-section of Q with medium quarks and gluons. In case of a Monte Carlo simulation this definition can be rewritten as:

$$\hat{q} = \frac{1}{l_x}\sum_{i=1}^{N_{coll}}(\Delta p_{T,i})^2 \qquad (12)$$

For $T = 350$ MeV and the probe charm energy of 16 GeV, we find $\hat{q}$ to be 1.2 GeV^2/fm with an uncertainty

of ± 0.2 GeV^2/fm, while for charm energy of 50 GeV $\hat{q}$ is calculated to be 1.1 GeV^2/fm with ± 0.3 GeV^2/fm uncertainty. Due to the rather large statistical uncertainty in our $\hat{q}$ extraction, we cannot make any statements regarding the energy-dependence of $\hat{q}$ at this time. Our results do suggest a range of values for $\hat{q}$ somewhere between 1–1.5 GeV^2/fm for the RHIC system.

In future studies, we will extend our work to the temperature dependence of the transport coefficient and energy-loss as well as to the heavy-quark energy dependence of these quantities. The ultimate goal of course will be the application of the PCM to heavy quark observables in ultra-relativistic heavy-ion collisions at the LHC.

IV. SUMMARY

The present work aims to validate the applicability of the Parton Cascade Model for the description of heavy quark evolution in a partonic medium. We have calculated collisional and radiative energy loss of heavy quarks in an infinite medium at fixed temperature and find good agreement between the PCM and analytical calculations for elastic energy loss, but some discrepancies regarding radiative energy loss, which can be understood in terms of the approximations made in the analytical calculations. This is a first important step towards applying the PCM to the production and evolution of heavy-quarks in a QGP, as produced in collisions of ultra-relativistic heavy-ions at RHIC and LHC.

Acknowledgments

[1] J. C. Collins and M. J. Perry, Phys. Rev. Lett. **34**, 1353 (1975); L. D. McLerran and B. Svetitsky, Phys. Lett. **B 98**, 195 (1981).

[2] K. Kajantie, C. Montonen and C. Pietarinen, Zeit. Phys. **C 9**, 253 (1981); R. Hagedorn and J. Rafelski, Phys. Lett. **B 97**, 180 (1980).

[3] J. W. Harris and B. Müller, Ann. Rev. Nucl. Part. Sci. **41**, 96 (1996); B. Müller, Rep. Prog. Phys. **58**, 611 (1998).

[4] S. A. Bass, M. Gyulassy, H. Stöcker and W. Greiner, J. Phys. **G**: Nucl. Part. Phys. **25**, R1 (1999).

[5] A. Drees, Nucl. Phys. **A 698**, 331 (2002); E. Shuryak, Nucl. Phys. **A 750**, 64 (2005); S. Jeon and G. D. Moore, Phys. Rev. **C 71**, 034901 (2005).

[6] X-N. Wang, Nucl. Phys. **A 750**, 98 (2005); A. K. Chaudhuri, Phys. Lett. **B 659**, 531 (2008); David d'Enterria and B. Betz, Lect. Notes Phys. **785**, 285 (2010).

[7] A. Adare et al. (PHENIX Collaboration), Phys. Rev. Lett. **98**, 172301 (2007); B. I. Abelev et al. Phys. Rev. Lett. **98**, 192301 (2007); B. Abelev et al (ALICE Collaboration), arXiv:1203.2160v1[nucl-ex]2012.

[8] G. Moore and D. Teaney, Phys. Rev. **C 71**, 064904 (2005); S. Cao and S. A. Bass, arXiv:1209.5405v1[nucl-th] 2012.

[9] S. Mazumder and J. Alam, Phys. Rev. **C 85**, 044918 (2012) and references therein.

[10] H. van Hees, M. Mannarelli, V. Greco and R. Rapp, Phys. Rev. Lett. **100**, 192301 (2008); H. van Hees and R. Rapp, Phys. Rev. **C 71**, 034907 (2005); H. van Hees, V, Greco and R. Rapp, Phys. Rev. **C 73**, 034913 (2006); M. He, R. J. Fries and R. Rapp, Phys. Rev. **C 86**, 014903 (2012).

[11] M. G. Mustafa, D. Pal and D. K. Srivastava, Phys. Rev. **C 57**, 889 (1998); C. M. Ko and W. Liu, Nucl. Phys. **A 783**, 23c (2007).

[12] Y. Akamatsu, T. Hatsuda and T. Hirano, Phys. Rev. **C 79**, 054907 (2009).

[13] S. Mazumder, T. Bhattacharyya, J. Alam, S. K. Das, Phys. Rev. **C 84**, 044901 (2011).

[14] S. Cao and S. A. Bass, J. Phys. **G**: Nucl. Part. Phys. **40**, 085103 (2013); arXiv:1209.5410[nucl-th]2012; M. Younus and D. K. Srivastava, J. Phys. G: Nucl. Part. Phys. **39**, 095003 (2012).

[15] P. B. Gossiaux, J. Aichelin, T. Gousset, Acta. Phys. Polon. **B 43**, 655 (2012); A. Meistrenko, A. Peshier, J. Uphoff, C. Greiner, Nucl. Phys. **A 901**, 51 (2013).

[16] K. Geiger and B. Müller, Nucl. Phys. **B 369**, 600 (1992); K. Geiger, Phys. Rev. **D 47**, 133 (1993); K. Geiger and D. K. Srivastava, Phys. Rev. **C 56**, 2718 (1997); D. K. Srivastava and K. Geiger, Phys. Lett. **B 422**, 39 (1998).

[17] B. Zhang, M. Gyulassy and C. M. Ko, Phys. Lett. **B 455**, 45 (1999).

[18] C. M. Ko, B-W. Zhang and L-W. Chen, J. Phys. **G 34**, S413 (2007); J. Uphoff, O. Fochler, Z. Xu and C. Greiner, Phys. Rev. **C 82**, 024907 (2010); O. Fochler, Z. Xu and C. Greiner, Phys. Rev. **C 82**, 044906 (2010).

[19] S. A. Bass, B. Müller and D. K. Srivastava, J. Phys. **G**: Nucl. Part. Phys., **30**, S1283 (2004); D. Y. Chang, S. A. Bass and D. K. Srivastava, J. Phys. **G**: Nucl. Part. Phys., **31**, S1005 (2005).

[20] G. R. Shin, S. A. Bass, B. Müller, J. Phys. G :Nucl. Part. Phys. **37**, 105112 (2010); C. E. Coleman-Smith, G-Y. Qin, S. A. Bass, arXiv:1108.5662v1[hep-ph]2011.

[21] C. E. Coleman-Smith, B. Müller, arXiv:1210.3377v1[hep-ph] 2012.

[22] B. L. Combridge, Nucl. Phys. **B 151**, 429 (1979); B. Svetitsky, Phys. Rev. **D 37**, 2484 (1988).

[23] N. Armesto et al., Phys. Lett. **B 637**, 362 (2006); H. Van Hees, V. Greco and R. Rapp, Phys. Rev. **C 73**, 034913 (2006); J. Uphoff, O. Fochler, Z. Xu and C. Greiner,

Acta. Phys. Pol. **B 5**, 555 (2012).

[24] M. Thoma and M. Gyulassy, Nucl. Phys. **B 351**, 491 (1991).

[25] P. B. Gossiaux and J. Aichelin, arXiv:0802.2525v2[hep-ph] 2008.

[26] G. Altarelli and G. Parisi, Nucl. Phys. **B 126**, 298 (1997); G. Altarelli, Phys. Rep. **81**, 1 (1982); M. Bengstonn and T.Sjöstrand, Nucl. Phys. **B**, 289, 810 (1987).

[27] H. Bethe and W. Heitler, Proc. Royal Soc. London, series A, **46**, 83 (1934); L. I. Schiff, Phys. Rev. **83**, 252 (1951); R. Baier, Y. L. Dokhshitzer, S. Peigne and L. I. Schiff, Phys. Lett. **B 345**, 277 (1995).

[28] R. Baier, Y. L. Dokhshitzer, A. H. Mueller, S. Peigne, and D. Schiff, Nucl. Phys. **B 478**, 577 (1996); R. Baier, Y. L. Dokhshitzer, A. H. Mueller, S. Peigne, and D. Schiff, Nucl. Phys. **B 483**, 291 (1997).

[29] Y. L.Dokhshitzer and D. E. Kharzeev, Phys. Lett. **B 519**, 199 (2001); R. Thoma,B. Kämpfer and G. Soff, arXiv:hep-ph/0465189v1, 2004.

[30] L. D. Landau and I. Pomeranchuk, Dokl. Akad. Nauk. Ser. Fiz. **92**, 535 (1953); Dokl. Akad. Nauk. Ser. Fiz. **92**, 735 (1953)(In Russian); A. B. Migdal, Phys. Rev. **103**, 6 (1956).

[31] R. Abir, C. Greiner, M. Martinez, M. G. Mustafa and J. Uphoff, Phys. Rev. D **85**, 054012 (2012).

[32] B-W. Zhang, E. Wang and X-N. Wang, Phys. Rev. Lett. **93**, 072301 (2004); M. G. Mustafa, D. Pal, D. K. Srivastava and M. H. Thoma, Phys. Lett. **B 428**, 234 (1998); Erratum, Phys. Lett. **B 438**, 450 (1998).

[33] K. C. Zapp, J. Stachel, U. A. Wiedemann, Nucl. Phys. **A 830**, 171c (2009).

[34] C. E. Coleman-Smith, S. A. Bass, D. K. Srivastava, Nucl. Phys. **A 862**, 275 (2011).

[35] P. B. Gossiaux, J. Aichelin, T. Gousset and V. Guiho, J. Phys. G **37**, 094019 (2010); J. D. Jackson, Classical Electrodynamics, 3rd Ed., John Wiley and Sons Pvt. Ltd.

[36] S. Cao, G-Y. Qin, S. A. Bass and B. Müller, Nucl. Phys. **A 904**, 653c (2013); F. Scardina, S. K. Das, S. Plumari, D. Perricone and V. Greco, J. Phys. Conf. Ser. **535**, 012019 (2014); S. K. Das, F. Scardina and V. Greco, "Heavy Flavor in Medium Momentum Evolution: Langevin vs Boltzmann," arXiv:1312.6857 [nucl-th] 2013.

[37] S. Peigné and A. Peshier, arXiv:0802.4362v1[hep-ph] 2008.

[38] R. Abir, U. Jamil, M. G. Mustafa, D. K. Srivastava, Phys. Lett. **B 715**, 183 (2012).

[39] R. Baier and Y. M-Tani, Phys. Rev. **C 78**, 064906 (2008).

[40] T. Renk, arXiv:1004.0809v1[hep=ph] 2010; C. E. Coleman-Smith and B. Müller, arXiv:1209.3328v1 [hep-ph] 2012.

[41] F. Arleo, JHEP **09**, 015 (2006); R. Baier and D. Schiff, JHEP **09**, 059 (2006).

[42] P. Romatschke, Phys. Rev. **C 75**, 014901 (2007).

[43] M. Gyulassy, P. Levai and I. Vitev, Phys. Rev. Lett. **85**, 26 (2000); Nucl. Phys. **B 571**, 197 (2001); Nucl. Phys. **B 594**, 371 (2001); N. Armesto, C. A. Salgado and U. A. Wiedemann, Phys. Rev. **D 69**, 114003(2004); F. D'Eramo, H. Liu and K. Rajagopal, Phys. Rev. **D 84**, 06015 (2011); A. Majumder, B. Müller and S. Mrówczyński, Phy. Rev. **D 80**, 125020 (2009); R. Baier, D. Schiff and B. G. Zakharov, Annu. Rev. Nucl. Part. Sci. **50**, 37 (2000); A. Kovner and U. A. Wiedemann, arXiv:hep-ph/0304152v1 2003; P. Arnold and W. Xiao, Phys. Rev. **D 78**, 125008 (2008).

[44] U. A. Wiedemann, arXiv:0908.2306v1[hep-ph] 2009; A. Majumder and M. Van Leeuwen, Prog. Part. Nucl. Phys. **66**, 41 (2011); S. Mazumder, T. Bhattacharyya and J. Alam, Phys. Rev. **D 89**, 014002 (2014).